p53 deletion rescues apoptosis and microcephaly in a Kif20b mouse mutant

Jessica Neville Little[1] and Noelle D. Dwyer[1,2]

[1] University of Virginia School of Medicine, Department of Cell Biology, Charlottesville, VA, USA

[2] Corresponding author. Email: ndwyer@virginia.edu

ABSTRACT

Development of the cerebral cortex requires precise divisions of neural stem cells (NSCs) that undergo symmetric and asymmetric divisions to produce post-mitotic neurons. One consequence of impaired embryonic NSC proliferation is microcephaly, or a small brain. Errors in NSC division are a common mechanism for microcephaly, resulting in slower proliferation, changes in cell fates, and/or cell death. While programmed cell death, or apoptosis, is increased in many mouse models of microcephaly, the mechanisms that control cell survival in NSCs are still not well understood. In a novel mouse model for microcephaly discovered by our lab, the mutation of the kinesin *Kif20b* results in reduced brain size at birth. Kif20b, previously known as Mphosph1, Mpp1 or KRMP1, regulates the last step of cytokinesis, abscission. After cleavage furrowing, the central spindle is compacted into the midbody, the last connection between two cells before the final separation, abscission. Midbody abnormalities and increased apoptosis were noted in *Kif20b-/-* embryonic brains. However, it was not known whether apoptosis was causative for the microcephaly, and whether it was a cell autonomous consequence of *Kif20b* loss in NSCs. To ascertain the contribution of apoptosis to *Kif20b-/-* microcephaly, we crossed the *Kif20b* mutant mouse to knockouts for the pro-apoptotic genes *Trp53* (encoding the tumor suppressor p53) and *Bax* to produce double mutants. We found that *Bax* deletion only partially rescues, but *p53* deletion fully rescues the embryonic apoptosis and microcephaly in *Kif20b* mutants. Interestingly, heterozygous deletion of *p53* provided the same amount of rescue as homozygous *p53* deletion. Finally, we demonstrated that midbody defects and apoptosis are both cell-autonomous consequences of Kif20b loss in NSCs. Thus, p53-dependent apoptosis in embryonic NSCs is the cause of microcephaly in *Kif20b-/-* mice. This adds to a growing body of evidence that p53 regulates cell survival decisions in embryonic NSCs, and also suggests that p53 responds to cytokinetic abscission defects in addition to other cell cycle defects. Future work will focus on determining the relationship between cytokinesis defects and p53 activation in *Kif20b-/-* mice and the consequences of abscission defects in *Kif20b-/- p53-/-* mice.

INTRODUCTION

Divisions of neural stem cells (NSCs), which produce the neurons and glia of the cerebral cortex, are tightly regulated in mammals during development. Defective NSC divisions can result in brain malformations including microcephaly, or a small brain (Bizotto and Francis 2015). Microcephaly can arise from many cellular defects including slowed or impaired NSC proliferation, an imbalance in the production of additional NSCs versus neurons from NSC divisions, neurite outgrowth defects, and/or cell death in NSCs or neurons (Gilmore and Walsh 2013, Faheem et al. 2015). While programmed cell death, or apoptosis, has been noted in many mouse models of human microcephaly

(Gilmore/Walsh 2013, Faheem et al. 2015), how cell survival decisions are made in individual NSCs and neurons is still poorly understood.

In the *Kif20b-/-* model of microcephaly, the forebrain is severely reduced in size, with decreased thickness of neuronal layers (Janisch, Vock et al. 2013). This mutant was discovered through an ENU screen for defective cortical development (Dwyer et al. 2011). Kif20b (also known as Mphosph1, MPP1 or KRMP1) is a plus-end directed microtubule motor in the Kinesin-6 family. Kinesin-6 family members, including Kif23 (MKLP1) and Kif20a (MKLP2), all have distinct roles in cytokinesis (Baron and Barr 2015). Interestingly, Kif20b is only found in vertebrate genomes and thus may have evolved with more complex nervous systems.

Kif20b regulates cytokinetic abscission. During cytokinesis, the cleavage furrow ingresses to form an intercellular bridge between two daughter cells, compacting the microtubules of the central spindle into a structure called the midbody. The midbody mediates the final separation of cells during division, a process termed abscission (Green et al., 2012; Mierzwa and Gerlich, 2014). Kif20b protein localizes to the central spindle and midbody, in human cell lines (Abaza et al. 2003, Kanehira et al. 2007, Janisch, McNeely et al 2018) as well as in dividing NSCs in the mouse cortex (Janisch, Vock et al. 2013). In human cells, Kif20b knockdown results in delayed or failed abscission (Abaza et al, 2003, Janisch, McNeely et al. 2018), and sometimes apoptosis (Abaza et al. 2003, Liu et al. 2014). Furthermore, in *Kif20b-/-* embryonic brains, NSC midbody abnormalities were observed (Janisch, Vock et al. 2013, Janisch et al. 2016). However, mitotic parameters and cleavage furrow angles were normal.

In addition to midbody abnormalities, apoptosis is increased 5-fold in *Kif20b-/-* cortex from embryonic age (E)10 to E16 (Janisch, Vock et al. 2013). Apoptosis is part of the normal development of many tissues, but also occurs in response to cell damage. There are two major pathways of apoptosis, the intrinsic or mitochondrial pathway, which responds to internal cellular defects, and the extrinsic or death receptor pathway, that mediates apoptotic signaling between cells (Elmore 2007). Whether a cell will undergo apoptosis following cell damage is cell and tissue type dependent (Wyles et al. 2014), and there is evidence that NSCs may be more susceptible to apoptosis than other cell types (Acharya et al. 2010, Nowak et al. 2006). Mitotic delay and DNA damage have been shown specifically to causes apoptosis in NSCs (Pilaz et al. 2016, Li et al. 2008). However, the molecular pathways that mediate the apoptotic response to cell division errors are only beginning to be elucidated. Whether other cell cycle defects, including impaired abscission, also cause apoptosis in NSCs remains to be determined.

We hypothesized that in the *Kif20b-/-* mouse, abscission defects lead to apoptosis in a subset of NSCs, depleting their number and hence the number of neuronal progeny, thereby causing microcephaly. Alternatively, microcephaly in the *Kif20b-/-* mutant could be due to slower NSC divisions, cell fate changes, and/or post-mitotic neurite outgrowth defects. Therefore, to test whether the small number of observed apoptotic cells could indeed account for the microcephaly, we sought to prevent apoptosis in the *Kif20b* mutant.

We attempted to inhibit apoptosis in the *Kif20b-/-* mouse by crossing to two mouse mutants for proteins involved in apoptotic pathways, *Trp53-/-* (referred to as *p53-/-* here; Jacks et al. 1994) and *Bax-/-* (Knudson et al. 1995). Notably, several microcephaly models with defects in other stages of the cell cycle have implicated p53 in the etiology of microcephaly (Insolera et al. 2014, Houlihan et al. 2014, Marjanovic et al. 2015, Marthiens et al. 2013, Bianchi et al 2017). However, it is not known whether p53 also responds to defects in abscission. While Bax is downstream of p53 and operates in both the intrinsic and extrinsic pathway of apoptosis (Westphal et al. 2011), a role for Bax in apoptosis of embryonic NSCs has not been demonstrated.

Finally, we sought to determine whether midbody defects and apoptosis were cell- autonomous consequences of *Kif20b* loss in NSCs. Culturing *Kif20b-/-* NSCs *in vitro* allowed us to determine which defects could be replicated *in vitro* and which were specific to the *in vivo* environment. This analysis revealed further insights into the consequences of *Kif20b* loss for NSC cytokinesis and cell survival.

Through this work we sought to determine whether *Kif20b-/-* NSCs would be able to successfully divide and build a cortex of correct size and structure if apoptosis was blocked. Investigating the contribution of apoptosis to this novel microcephaly model gives us insight into how NSC divisions are regulated to form a brain of normal size and structure.

RESULTS

Apoptosis is the key driver of microcephaly in *Kif20b-/-* brains

First, we investigated whether Bax is required for the apoptosis in *Kif20b-/-* mice by crossing the Kif20b mutant to the *Bax* mutant (Knudson et al. 1995), to produce mice double mutant for *Kif20b* and *Bax* (*Kif20b-/- Bax-/-).* Bax increases the permeability of the mitochondrial membrane, increasing cytochrome c release, and can be activated by proteins in both the extrinsic and intrinsic apoptotic pathways (Westphal et al. 2011). At E14.5, the craniofacial abnormalities previously noted in *Kif20b-/-* mice did not appear to be rescued in *Kif20b-/- Bax-/-* mice (data not shown). However, by careful analysis we determined that *Bax* deletion partially rescued both cortical thickness (**Figure 1A-D**) and apoptosis by cleaved-caspase 3 (CC3) labeling (**Figure 1E-H**) at E14.5. Therefore, other proteins must also be involved in the apoptotic response to *Kif20b* loss. However, this data shows that the amount of apoptosis and the severity of microcephaly are strongly correlated, and that apoptosis activation is a key driver of microcephaly in *Kif20b-/-* mice.

The tumor suppressor p53 operates upstream of Bax and is a master regulator of the intrinsic apoptotic pathway. To determine the role of p53 in *Kif20b-/-* microcephaly, we first examined total p53 protein expression by immunoblot of E12.5 cortical lysates. We found a 50% increase in p53 expression in *Kif20b-/-* samples normalized to beta-catenin. As beta-catenin is more highly expressed in NSCs than neurons (Chenn and Walsh 2002), this controlled for the relative amounts of NSCs and neurons in control and *Kif20b-/-* samples (**Supp. Figure 1A**). Next, we crossed the *Kif20b* mutant mouse line to the *Trp53-/-* mouse line (Jacks et al. 1995) to produce mice double mutant for *Kif20b* and *p53* (*Kif20b-/- p53-/-*). Strikingly, by comparing matching coronal sections at E14.5, we determined that both heterozygous and homozygous *p53* deletion rescued the decreased cortical thickness in *Kif20b-/-* mice (**Figure 1I-M**). Furthermore, layering by H&E stain appeared grossly normal in *Kif20b-/-* mice with either heterozygous or homozygous *p53* mutation (**Figure 1I-L**). Additionally, compared to *Kif20b-/-* single mutant mice, which exhibited craniofacial abnormalities including, with variable penetrance, protruding tongue, cleft palate and underdeveloped eyes, *Kif20b-/- p53+/-* and *Kif20b-/- p53-/-* mice showed none of these craniofacial abnormalities (**Supp. Figure 2A-E**). However, as previously reported approximately 1/10 *p53-/-* mice displayed exencephaly (Sah et al. 1995), as did a similar ratio of *Kif20b-/- p53-/-* mice (data not shown).

We next sought to determine if this rescue by *p53* deletion was through inhibition of apoptosis. Indeed, by labeling sections with CC3, we discovered that the increased apoptosis in *Kif20b-/- p53+/+* mice was rescued by heterozygous or homozygous *p53* deletion (**Figure 1N-R**). The rescue of apoptosis by halving the amount of p53 indicates that two functional copies of p53 are required to produce apoptosis and subsequent microcephaly in the *Kif20b* mutant.

_p53_ deletion restores normal production of intermediate progenitors and neurons in _Kif20b-/-_ cortex

During corticogenesis, neural stem cells divide symmetrically and asymmetrically to produce both intermediate progenitors and neurons. Intermediate progenitors can then divide an additional time to produce two neurons (Pontious et al. 2008). The reduced cortical thickness in *Kif20b-/-* brains is primarily due to thinner neuronal layers. At E14.5, the neuronal layer is proportionately thinner, and the ventricular zone (where NSCs reside), is proportionately thicker than controls. Additionally, the number of intermediate progenitors is reduced (Janisch, Vock et al. 2013). While *p53* deletion rescued the overall cortical thickness in *Kif20b-/-* mice, we were interested to see if neurogenesis and the cortical structure of *Kif20b-/- p53-/-* mice would be normal. To investigate cortical structure in more detail, we labeled sections with antibodies to Pax6, to label NSCs, Tbr2, to label intermediate progenitors, and Tuj1, to label neurons. In *Kif20b-/- p53+/+* mice, as expected, the ventricular layer where Pax6+ NSCs reside was proportionately thicker, the Tuj1+ neuronal layer was proportionately thinner compared to control, and the number of Tbr2+ intermediate progenitors was reduced (**Figure 2B and 2E**). Remarkably, *Kif20b-/- p53-/-* mutant mice had normal generation and layering of neurons, indistinguishable from controls (**Figure 2A-C, G**). Additionally, *Kif20b-/- p53-/-* mice had normal generation of intermediate progenitors and the ventricular zone thickness was comparable to controls (**Figure 2D-F, H-I**). Therefore, blocking apoptosis restored cortical thickness by rescuing sufficient production of neurons and intermediate progenitors in *Kif20b-/-* mice.

Kif20b is required cell-autonomously for cytokinesis of cortical NSCs

Based on our previous work documenting Kif20b's role in abscission, and the preceding data that shows the centrality of p53 an apoptosis to the microcephaly phenotype, we hypothesized that abscission defects in NSCs trigger intrinsic apoptosis. Alternatively, it is also possible that midbody defects and/or apoptosis are not cell-autonomous *in vivo* because cytokinesis in epithelia is considered a multicellular process (Herszterg et al. 2014). Therefore, to test whether Kif*20b* loss triggers cytokinesis defects and apoptosis cell-autonomously in NSCs we made primary cortical cell cultures *in vitro*.

We first tested whether midbody defects were seen in isolated *Kif20b-/-* NSCs from E12.5 cortices *in vitro*, as abnormalities in abscission have been noted upon Kif20b knockdown in other cell lines (Janisch, McNeely et al. 2018) as well as in *Kif20b-/-* cortex (Janisch, Vock et al. 2013, Janisch et al. 2016). Midbodies can be detected with Aurora B kinase (AurkB) staining in NSCs by their characteristic shape (**Figure 3A-C, A'-C'**). Early stage midbodies that form after cleavage furrowing, are wider (**Figure 3A, A'**). As the midbody matures in preparation for abscission, the midbody becomes thinner (**Figure 3B, B'**). Next, constriction sites form, the sites of future abscission, when the daughter cells are finally cleaved apart (**Figure 3B, B', C, C'**) (Mierzwa and Gerlich et al. 2014). Constriction sites are more readily detected with alpha-tubulin immunostaining (**Figure 3A-C**) than AurkB immunostaining (**Figure 3A'-C'**). Interestingly, in *Kif20b-/-* cultures, there are increased NSCs with midbodies that have no constriction sites, and decreased numbers of NSCs with midbodies that have 1 or 2 constriction sites (**Figure 3D**). Additionally, midbodies in *Kif20b-/-* NSC cultures have an altered shape distribution, with more wide midbodies observed, as determined by measuring the width of AurkB protein expression (**Figure 3E**). This distribution of midbody stages suggests that *Kif20b-/-* NSCs have a defect in midbody maturation, both in the narrowing stage that occurs after cleavage furrowing and in the formation of constriction sites.

Next, we addressed whether *Kif20b* mutant NSCs spent more time in mitosis or abscission than control NSCs by determining the proportion of proliferating NSCs (Ki67+) in mitosis (Ph3+) or midbody stages. Surprisingly, in *Kif20b* mutant cultures, there were decreased proportions of NSCs in both mitosis and at the midbody stage (**Figure 3G**). This could suggest that either mitosis and abscission occur faster in the *Kif20b* mutant NSCs, or that mutant NSCs are arrested or dying. To analyze this further, we categorized all mitotic or midbody stage cells into sub-stages of mitosis and cytokinesis by appearance of PH3 and AurkB staining (**Figure 3F**). We found an altered distribution of mitotic and cytokinetic stages in *Kif20b-/-* cultures (**Figure 3H**), with an increased proportion in anaphase and early telophase in *Kif20b-/-* cultures. This may indicate *Kif20b-/-* NSCs are delayed in this stage of division compared to other stages, perhaps due to slower midbody formation.

***Kif20b* loss activates apoptosis cell-autonomously in proliferating cortical NSCs**

Having established that *Kif20b* loss causes cell-autonomous defects in cytokinesis, we wanted to test whether it also causes apoptosis cell-autonomously. We evaluated CC3 expression in control and mutant cultures after 24 hours *in vitro,* and found that apoptosis is elevated in *Kif20b-/-* NSCs more than two-fold (**Figure 4A-B, E**). To determine if apoptotic cells were neural stem cells or neurons, we co-labeled cells with Nestin, Tuj1, and Ki67. Interestingly, there were increased numbers of apoptotic NSCs, but not apoptotic neurons, in *Kif20b* mutant cultures (**Figure 4C-D,F**). Furthermore, there were increased numbers of apoptotic cells among cycling NSCs (co-positive for CC3 and Ki67) (**Figure 4F**). This may explain why fewer cycling NSCs were seen in mitosis and cytokinesis (**Figure 3G**), as a proportion of them are undergoing apoptosis. These data indicate that not only is apoptosis a cell-autonomous consequence of *Kif20b* loss for NSCs, but that apoptosis occurs specifically in cycling NSCs, not neurons.

DISCUSSION

Here, we have demonstrated that apoptosis is the primary cause of microcephaly in the *Kif20b-/-* mouse. We were successful in partially inhibiting apoptosis with the *Bax* mutant, and fully blocking apoptosis with the *p53* mutant. Interestingly, Bax and p53 knockouts rescued *Kif20b-/-* brain size in direct proportion to the degree of apoptosis inhibition. Surprisingly, in addition to rescue of overall brain size, *Kif20b-/-; p53-/-* neural stem cells were able to produce intermediate progenitors and neurons that migrated correctly to their proper layers. These data indicate that apoptosis is the key driver of the microcephaly phenotype in *Kif20b-/-* mice, and this apoptosis requires p53 activation.

Rescue of *Kif20b-/-* microcephaly by *p53* co-deletion adds to a growing body of work that implicates p53 in the regulation of NSC proliferation. Other microcephaly models with defects in mitosis and S phase have been partially or completely rescued by p53 deletion as well (Insolera et al. 2014, Houlihan et al. 2014, Marjanovic et al. 2015, Marthiens et al. 2013). Microcephaly in the citron kinase mouse mutant, which has defects in early cytokinesis as well as DNA repair, is partially rescued by *p53* co-deletion (Bianchi et al. 2017). Recently, cytokinetic defects have been found in human patients with microcephaly, but whether the small brain size in these patients is caused by p53-dependent apoptosis is not yet known (Harding et al. 2016, Li et al. 2016, Frosk et al. 2017, Periklis et al. 2018) Furthermore, Zika virus infection was recently shown to result in p53-dependent apoptosis in human NSCs (Ghouzzi et al. 2016). Our work furthers the evidence that p53 responds to multiple cellular defects to acutely regulate cell survival in NSCs. However, the novel phenotypes in this mutant, specifically of defects in the late

stages of cytokinesis, abscission, suggest that p53 may have even greater surveillance of cell division defects than previously appreciated.

Surprisingly, *Kif20b-/-* microcephaly was rescued by even heterozygous deletion of *p53*. This interesting finding indicates that the microcephaly in *Kif20b-/-* mice is tightly controlled by p53 activation, with activation of apoptosis only when two *p53* copies are present. Rescue by heterozygous deletion of *p53* has not been reported in other microcephaly mutants but was in the case of dwarfism in the BRCA1 mutant (Xu et al. 2001). It has been reported that the number of *p53* copies correlates with the strength of the apoptotic response in a dose-dependent manner (Xu et al. 2001). The *Kif20b-/-* microcephaly model is more severe in reduction of brain size compared to some other models, but it is also more rescuable- by partial p53 inhibition. This suggests that p53-dependent apoptosis may be activated by a distinct molecular mechanism in the *Kif20b-/-* mutant compared to other models.

Interestingly, *Bax* deletion partially rescued both apoptosis and microcephaly in *Kif20b-/-* mice. Bax can operate both downstream of p53 in the intrinsic pathway and downstream of caspase-8 in the extrinsic pathway (Westphal et al. 2011). Therefore, the partial rescue of apoptosis by *Bax* deletion indicates that other proteins also operate downstream of p53 in the apoptotic pathway following *Kif20b* loss, possibly the Bax family member Bak (Westphal et al. 2011). Still, these data indicate that Bax responds to impaired cell division in the embryonic cortex. Additionally, the close correlation between extent of apoptosis rescue and extent of brain size rescue by *Bax* and *p53* deletions shows that apoptosis is the main driver of microcephaly in *Kif20b-/-* mice.

Importantly, we have demonstrated that cytokinetic defects are cell-autonomous consequences of *Kif20b* loss in NSCs cultured *in vitro.* The increased frequency of wider midbodies and decreased frequency of constriction sites in *Kif20b-/-* NSCs suggests that Kif20b is needed for midbody maturation. These data are consistent with findings in HeLa cells that Kif20b knockdown results in midbodies with decreased constriction sites and decreased markers of late abscission stages (Janisch, McNeely et al. 2018). Data from postmitotic neurons supports the notion that a key function of Kif20b is to enable tight microtubule packing: in *Kif20b* mutant neurons wider neurites with gaps in microtubule bundles were noted (McNeely, Cupp et al. 2017). Additionally, Kif20b has microtubule crosslinking activity *in vitro* (Abaza et al. 2003). Therefore, Kif20b may help to bundle microtubules in both NSCs and neurons.

We have also determined that apoptosis is a cell-autonomous consequence of *Kif20b* loss in NSCs. A priori, it was possible that apoptosis may have only arisen in the *in vivo* environment, from a non-cell-autonomous requirement for Kif20b. However, apoptosis is increased more than two-fold in dissociated cortical cell cultures after 24 hours. Additionally, we found that apoptosis was increased in proliferating NSCs, but not neurons. Therefore, apoptosis is linked with and likely occurs due to errors in cell division in *Kif20b-/-* NSCs. Given that midbody defects but no other abnormalities were observed in dissociated *Kif20b-/-* NSCs, we hypothesize that apoptosis is a consequence of cytokinetic errors upon *Kif20b* loss.

Our data suggest a novel pathway for p53 activation, in responding to abscission defects in addition to previously reported cell cycle errors. We propose the following working model: delayed or defective abscission in *Kif20b-/-* NSCs activates p53, which in turn activates the apoptotic cascade including Bax activation in proliferating NSCs. Cell death depletes the neural stem cell pool, resulting in decreased production of neurons and smaller brain size. Notably, there may be some stochasticity to this process, as not all *Kif20b-/-* NSCs have midbody defects, and only a small percentage undergo apoptosis (Janisch, Vock et al. 2013, this work). In the context of mitotic delay, the likelihood of apoptosis increases with the amount of time spent in mitosis (Pilaz et al.

2016), which may be similar in the case of cytokinetic defects. An alternative possibility to our current model is that the midbody defects we have noted are downstream of p53 activation, and that p53 responds to another, as yet unidentified defect in *Kif20b-/-* NSCs. A third possibility is that *Kif20b* loss causes midbody defects independently of p53 activation. Future work will distinguish between these possible pathways. Finally, while *Kif20b-/- p53-/-* mice have rescued brain size and overall cortical structure, we will continue to investigate possible consequences of abnormal abscission for corticogenesis in these mice.

MATERIALS AND METHODS

Mice: Mouse colonies were maintained in accordance with NIH guidelines and policies approved by the IACUC. Embryos were harvested by caesarean section, and the morning of the vaginal plug was considered embryonic day (E) 0.5. Littermate embryos served as controls for all experiments. The *magoo* mutation, as previously described (Janisch, Vock et al. 2013) is maintained on both BL6 and FVB/N backgrounds, and mixed background embryos are used for experiments. $Trp53^{tm1Tyj}$ mice were obtained from The Jackson Laboratory (JAX stock #002101) (Jacks et al. 1994). Bax^{tm1Sjk} mice were a gift from Christopher Deppmann (JAX stock #002994) (Knudson et al. 1995).

Preparation of Cryosections: For IHC experiments on cortical sections, age E14.5 brains were removed from heads and fixed for 6 hours in 4% PFA, followed by immersion in 30% sucrose in PBS overnight. Next, whole brains were embedded in OTC (Tissue-Tek, 4583) and cryosections were cut at 20 µm thickness and collected on Superfrost Plus slides (Fisher Scientific, 12-550-15).

Cortical cell cultures: Cells were dissociated from E12.5 cortices following a protocol adapted from Sally Temple's lab (Qian et al., 1998). The Worthington Papain Dissociation Kit was used to dissociate cells (Worthington Biochemical Corporation, Cat # LK003150). Cells were cultured in DMEM with Na-Pyruvate, L-Glutamine, B-27, N2, N-acetyl-cysteine and basic Fibroblast Growth Factor (bFGF). After 24 hours, cells were fixed by adding an equal volume of room-temperature 8% PFA for 5 minutes to cell media, followed by removal of media and addition of -20º cold methanol for 5 minutes.

Immunoblotting: Brain lysates were prepared with RIPA lysis buffer (150 mM NaCl, 1% NP40, 0.5% sodium deoxycholate, 0.1% SDS, 50 mM Tris-HCl pH 8) with protease and phosphatase inhibitors. Protein concentration in lysates was determined by bicinchoninic acid (BCA) assay, and 60 µg total protein was loaded per lane on 4-20 gradient% polyacrylamide gels. Proteins were transferred by electroblotting onto a 0.2 µm PVDF membrane overnight at 30 mA. Membranes were blocked in 150 mM NaCl, 100 mM Tris-HCl pH 7.5 and 0.5% Tween 20 (TBST) with 5% dried milk (blocking buffer) for 1 hour. Primary antibodies were incubated with the membrane overnight at 4°C. After three washes, LI-COR IRDye 800 CW goat anti-rabbit IgG and 680 RD goat anti-mouse secondary antibodies were applied (1:10000) in blocking buffer for 1 hour at room temperature. After washing with TBST for 5 minutes, 3 times, immune complexes were visualized using a LI-COR western blot imager.

Immunostaining: For IHC on cryosections, sections were warmed to room temperature, then immersed in 10 mM citrate buffer at 95 degrees for 20 minutes. After cooling, sections were blocked in 2% NGS for 1 hour, followed by incubation with primary

antibodies overnight at 4º C. The next day, after PBS washes sections were incubated with AlexaFluor secondary antibodies at 1:200 and DAPI at 1:100 for 30 minutes followed by PBS washes and coverslipping with VectaShield fluorescent mounting medium (Vector Laboratories Inc., H-1000). For IF on coverslips of dissociated cortical progenitors, a similar protocol was used but with primary antibodies applied for 3 hours at room temperature, and antigen retrieval was not used. Coverslips were mounted on Superfrost Plus slides with Fluoro-Gel (Electron Microscopy Sciences, 17985-10).

Antibodies: Antibodies used in this analysis were cleaved-caspase 3 (Cell-Signaling 9661S, rabbit, 1:250), beta-III-tubulin (Tuj1) (BioLegend 801201, mouse, 1:500), Tbr2 (eBioscience 14-4875, rat, 1:200), Pax6 (BioLegend PRB-278P, rabbit, 1:200), Aurora b kinase (BD Biosciences 611082, mouse, 1:300), alpha-tubulin (Thermo Scientific RB-9281-P0, rabbit, 1:300), alpha-tubulin (Novus Biologicals NB600-506, rat, 1:300), PH3 (Cell Signaling 3458, rabbit, 1:200), Nestin (Aves Labs NES, chick, 1:600), Ki67 (eBioscience 14-5698, rat, 1:100) and p53 (Millipore PO4637, mouse, 1:250) and Beta-Catenin (Sigma CL15B8 rabbit, 1:1000).

Imaging, Analysis and Statistics: Images were collected on either a Zeiss Axio ImagerZ1 microscope with AxioCam MRm, a Zeiss AxioObserver fluorescent widefield inverted scope microscope, or a Leica MZ16F microscope with DFC300FX camera. **Control and mutant fluorescence images were collected with the same exposure times and on the same day.** All image analysis was performed in ImageJ and any changes to brightness and contrast were applied uniformly across images. Statistical analyses were performed using Excel (Microsoft) or GraphPad PRISM software. Statistical tests used are specified in each figure legend.

ACKNOWLEDGEMENTS

We thank Chris Deppmann for use of the *Bax* mutant mouse line. We are grateful to Katrina McNeely and Yuanyi Feng, as well as Bettina Winckler, Jing Yu, Xiaowei Lu, Ann Sutherland, Todd Stukenberg and members of their labs for advice and discussion. We thank Gabrielle Wolfe, Mackenzie Shannon and Haley Hopkinson for help with cryosectioning and data analysis. This work was supported by the National Institutes of Health (R01 NS076640 to NDD), the UVA Medical Scientist Training Program (MSTP T32 GM 7267-37) and the UVA Cell and Molecular Biology Training Grant (2T32GM008136-31A1).

REFERENCES

Abaza A, Soleilhac JM, Westendorf J, Piel M, Crevel I, Roux A, Pirollet F: **M phase phosphoprotein 1 is a human plus-end-directed kinesin-related protein required for cytokinesis**. *J Biol Chem* 2003, **278**(30):27844-27852.

Acharya MM, Lan ML, Kan VH, Patel NH, Giedzinski E, Tseng BP, Limoli CL. *Consequences of ionizing radiation-induced damage in human neural stem cells.* **Free Radical Biology and Medicine** 2010, 49(12): 1846-1855.

Baron RD, Barr FA. **The Kinesin-6 Members MKLP1, MKLP2 and MPP1.** In: Kozielski, FSB F. (eds) *Kinesins and Cancer* 2015. Springer, Dordrecht

Bianchi FT, Tocco C, Pallavicini G, Liu Y, Verni F, Merigliano C, Bonaccorsi S, El-Assawy N, Priano L, Gai M, Berto GE, Chiotto AM, Sgro F, Caramello A, Tasca L, Ala U, Neri F, Oliviero S, Mauro A, Geley S, Gatti M, Di Cunto F. **Citron Kinase Deficiency Leads to Chromosomal Instability and TP53-Sensitive Microcephaly.** *Cell Reports* 2017, 18(7): 1674-1686.

Bizotto S. and Francis F. **Morphological and functional aspects of progenitors perturbed in cortical malformations.** *Frontiers in Cellular Neuroscience* 2015, **9**:30.

Chenn A, Walsh CA. **Regulation of cerebral cortical size by control of cell cycle exit in neural precursors.** *Science* 2002, 297(5580): 365-9.

Dwyer ND, Manning DK, Moran JL, Mudbhary R, Fleming MS, Favero CB, Vock VM, O'Leary DD, Walsh CA, Beier DR: **A forward genetic screen with a thalamocortical axon reporter mouse yields novel neurodevelopment mutants and a distinct Emx2 mutant phenotype**. *Neural Dev* 2011, **6**(1):3.

Elmore S. **Apoptosis: A review of programmed cell death.** *Toxicol Pathol.* 2007, 35(4): 495-516.

Faheem M, Naseer MI, Rasool M, Chaudhary AG, Kumosani TA, Ilyas AM, Pushparaj PN, Ahmed F, Algahtani HA, Al-Qahtani MH, Jamal HS. **Molecular genetics of human primary microcephaly: an overview.** *BMC Med Genomics* 2015, 8(Suppl1): S4.

Frosk P, Arts HH, Philippe J, Gunn CS, brown EL, Chodirker B, Simard L, Majewski J, Fahiminiya S, Russell C, Liu YP, Hegele R, Katsanis N, Goerz C, Del Bigio MR, Davis EE. **A truncating mutation in CEP55 is the likely cause of MARCH, a novel syndrome affecting neuronal mitosis.** *J Med Genetics* 2017, 54(7): 490-501.

Gilmore EC, Walsh CA. **Genetic causes of microcephaly and lessons for neuronal development.** *Wiley Interdiscip Rev Dev Biol* 2013, 2(4): 461-78. 2013

Ghouzzi VE, Bianchi FT, Molineris I, Mounce BC, Berto GE, Rak M, Lebon S, Aubry L, Tocco C, Gai M, Chiotto AM, Sgro F, Pallavicini G, Simon-Loriere E, Passemard S, Vignuzzi M, Gressens P and Di Cunto F. **ZIKA virus elicits P53 activation and genotoxic stress in human neural progenitors similar to mutations involved in severe forms of genetic microcephaly.** *Cell Death Dis* 2016, **7**(10):e2440.

Green RA, Paluch E, Oegema K: **Cytokinesis in animal cells**. *Annual review of cell and developmental biology* 2012, **28**:29-58.

Harding BN, Moccia A, Drunat S, Soukarieh O, Tubeuf H, Chitty LS, Verloes A, Gressens P, El Ghouzzi V, Joriot S, Di Cunto F, Martins A, Passemard S, Bielas SL: **Mutations in Citron Kinase Cause Recessive Microlissencephaly with Multinucleated Neurons**. *Am J Hum Genet* 2016, **99**(2):511-520.

Herszterg S, Pinheiro D, Bellaiche Y. **A multicellular view of cytokinesis in epitheial tissue.** *Trends Cell Biol* 2014, 25(5): 285-93.

Houlihan S and Feng Y. **The scaffold protein Nde1 safeguards the brain genome during S phase of early neural progenitor differentiation**. *Elife* 2014, **3**:e03297.

Insolera R, Bazzi H, Shao W Anderson KV, Shi SH. **Cortical neurogenesis in the absence of centrioles.** *Nature Neuroscience* 2014, **17**(11): 1528-35.

Janisch KM, Vock VM, Fleming MS, Shrestha A, Grimsley-Myers CM, Rasoul BA, Neale SA, Cupp TD, Kinchen JM, Liem KF, Jr., Dwyer ND: **The vertebrate-specific Kinesin-6, Kif20b, is required for normal cytokinesis of polarized cortical stem cells and cerebral cortex size**. *Development* 2013, **140**(23):4672- 4682.

Jacks T, Remington L, Williams BO, Schmitt EM, Halachmi S, Bronson RT, Weinberg RA. **Tumor spectrum analysis in p53-mutant mice.** *Current Biology* 1994, 4(1): 1-7.

Janisch KM, Dwyer ND: **Imaging and quantitative analysis of cytokinesis in developing brains of Kinesin-6 mutant mice**. *Methods in cell biology* 2016, **131**:233-252.

Janisch KM, McNeely KC, Dardick JM, Lim SH, Dwyer ND. **Kinesin-6 KIF20B is required for efficient cytokinetic furrowing and timely abscission in human cells.** *Mol Biol Cell* 2018, 29(2): 166-179.

Kanehira M, Katagiri T, Shimo A, Takata R, Shuin T, Miki T, Fujioka T, Nakamura Y. **Oncogenic role of MPHOSPH1, a cancer-testis antigen specific to human bladder cancer.** *Cancer Research* 2007, **67**(7): 3276-85.

Knudson CM, Tung KS, Tourtellotte WG, Brown GA, Korsmeyer SJ. **Bax-deficient mice with lymphoid hyperplasia and male germ cell death.** *Science* 1995, 270(5233): 96-9.

Li H, Liu N, Rajendran GK, Gernon TJ, Rockhill JK, Schwartz JL, Gu Y. **A role for endogenous and radiation-induced DNA double-strand breaks in p53-dependent apoptosis during cortical neurogenesis**. *Radiat Res*. 2008 May; **169**(5): 513-22.

Li H, Bielas SL, Zaki MS, Ismail S, Farfara D, Um K, Rosti RO, Scott EC, Tu S, Chi NC, Gabriel S, Erson- Omay EZ, Ercan-Sencicek AG, Yasuno K, Caglayan AO, Kaymakcalan H, Ekici B, Bilguvar K, Gunel M, Gleeson JG: **Biallelic Mutations in Citron Kinase Link Mitotic Cytokinesis to Human Primary Microcephaly**. *Am J Hum Genet* 2016, **99**(2):501-510.

Liu X, Zhou Y, Liu X, Peng A, Gong H, Huang L, Ji K, Peterson RB, Zheng L, Huang K. **MPHOSPH1: a potential therapeutic target for hepatocellular carcinoma.** *Cancer Research* 2014, 74(22): 6623-24.

Marjanovic M, Sanchez-Huertas C, Terre B, Gomez R, Scheel JF, Pacheco S, Knobel PA, Martinez-Marchal A, Aivio S, Palenzuela L, Wolfrum U, McKinnon PJ, Suja JA, Roig I, Costanzo V, Luders J, Stracker TH. **CEP63 deficiency promotes p53-dependent microcephaly and reveals a role for the centrosome in meiotic recombination.** *Nature Communications* 2015, **6**:7676.

Marthiens V, Rujano MA, Pennetier C, Tessier S, Paul-Gilloteaux P, Basto R: **Centrosome amplification causes microcephaly**. *Nat Cell Biol* 2013, **15**(7):731-740.

Nowak E, Etienne O, Millet P, Lages CS, Mathieu C, Mouthon MA, Boussin FD. **Radiation-induced H2AX phosphorylation and neural precursor apoptosis in in the developing brain of mice.** *Radiation Research* 2006, 165(2): 155-64.

McNeely KC, Cupp TD, Little JN, Janisch KM, Shrestha A, Dwyer ND. **Mutation of Kinesin-6 Kif20b causes defects in cortical neuron polarization and morphogenesis.** *Neural Development* 2017, 12:5.

Pilaz LJ, McMahon JJ, Miller EE, Lennox AL, Suzuki A, Salmon E, Silver DL. **Prolonged Mitosis of Neural Progenitors Alters Cell Fate in the Developing Brain.** *Neuron* 2016, 89(1): 83-99.

Periklis M, Maroofian R, Stray-Pederson A, Musaev D, Zaki MS, Mahmoud IG, Selim L, Elbadawy A, Jhangiani SN, Akdemir ZHC, Gambin T, Sorte HS, Heiberg A, McEvoy-Venneri J, James KN, Stanley V, Belandres D, Guipponi M, Santoni FA, Ahangari N, Tara F, Doosti M, Iwaszkiewicz J, Zoete V, Backe PH, Hamamy H, Gleeson JG, Lupski JR, Karimiani EG, Antonarakis SE: **Biallelic variants in *KIF14* cause intellectual disability with microcephaly.** *European Journal of Human Genetics* 2018.

Pontious A, Kowalczyk T, Englund C, Hevner RF. **Role of intermediate progenitor cells in cerebral cortex development.** *Dev Neurosci.* 2008, 30(1-3): 24-32.

Zian X, Goderie SK, Shen Q, Stern JH, Temple S. **Intrinsic programs of patterned cell lineages in isolated vertebrate CNS ventricular zone cells**. *Development* 1998, 125 (3143-3152).

Sah VP, Attardi LD, Mulligan GJ, Williams BO, Bronson RT, Jacks T. **A subset of p53-deficient embryos exhibit exencephaly.** *Nature Genetics* 1995, 10:175-180.

Westphal D, Dewson G, Czabotar PE, Kluck RM. *Molecular biology of Bax and Bak activation and action.* **Biochemica et Biophysica Acta (BBA) – Molecular Cell Research** 2011, 1813(4): 521-531.

Wyles SP, Brandt EB, Nelson TJ. **Stem Cells: The Pursuit of Genomic Stability.** *International Journal of Molecular Sciences* 2014, 15(11): 20948-20967.

Xu X, Qiao W, Linke SP, Cao L, Li W, Furth PA, Harris CC, Deng C. **Genetic interactions between tumor suppressors Brca1 and p53 in apoptosis, cell cycle and tumorigenesis.** *Nature Genetics* 2001, 28,266-271.

Figure 1: Apoptosis is the key driver of microcephaly in *Kif20b-/-* brains

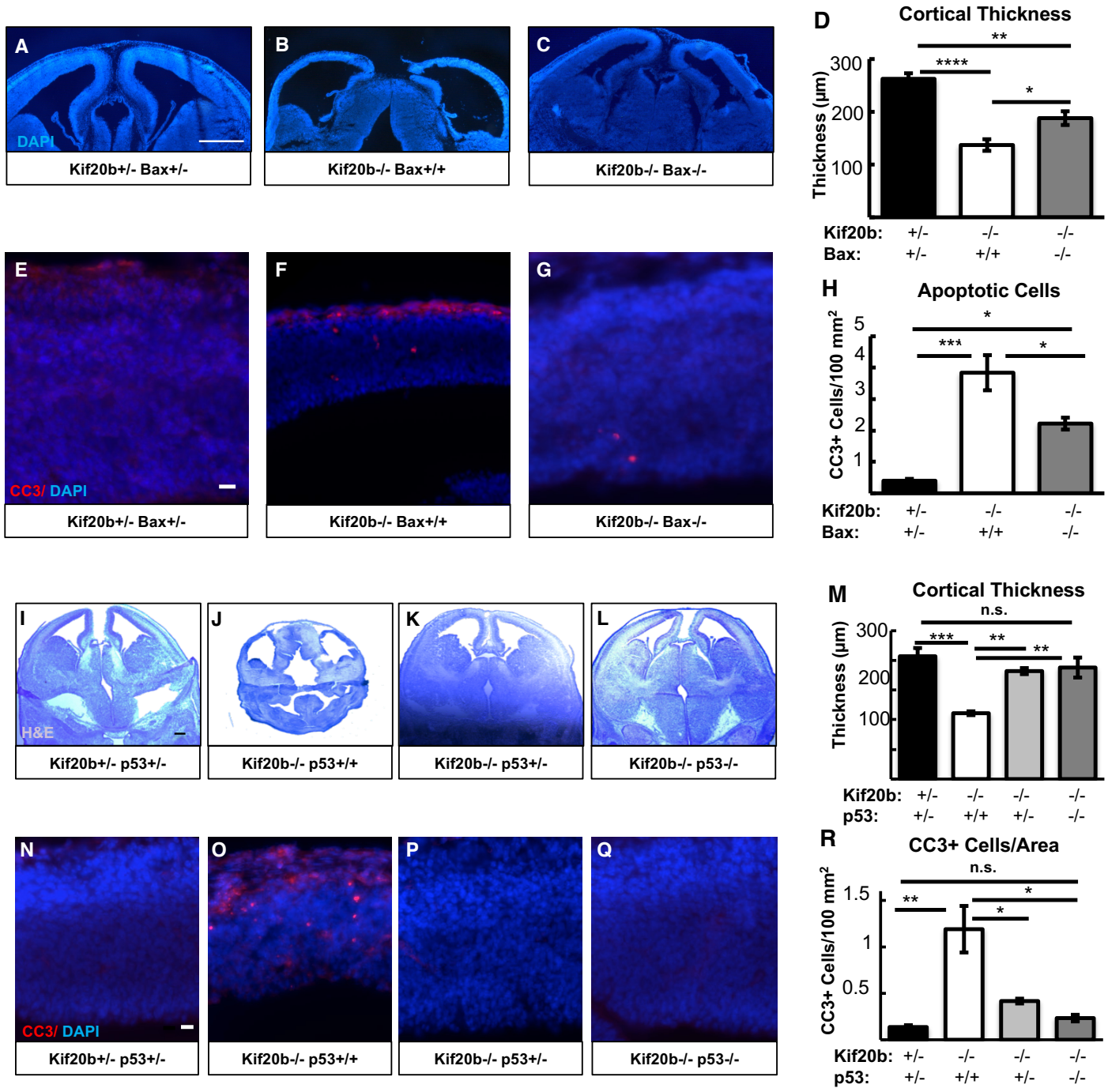

Figure 1: Apoptosis is the key driver of microcephaly in *Kif20b-/-* brains

(A-H) Bax deletion partially rescues microcephaly and apoptosis in *Kif20b-/-* brains.

A-C. Coronal sections from E14.5 brains of the indicated genotypes show cortical thickness is severely reduced in *Kif20b* single mutants, and partly restored in Kif20b;Bax double mutants. Scale bar: 500 µm.

D. The mean cortical thickness in controls, *Kif20b* single mutants, and Kif20b;Bax double mutants is shown. N = 5 *Kif20b+/- Bax+/-,* 4 *Kif20b-/- Bax+/+* and 5 *Kif20b-/- Bax-/-* mice.

E-G. Staining for CC3 in cortical sections from E14.5 brains of the indicated genotypes shows increased apoptosis in Kif20b single mutants is partially reduced in Kif20b;Bax double mutants. Scale bar: 20 µm.

H. Average apoptotic cell density in controls, *Kif20b* single mutants, and Kif20b;Bax double mutants is shown. N = 5 *Kif20b+/- Bax+/-,* 4 *Kif20b-/- Bax+/+* and 5 *Kif20b-/- Bax-/-* mice.

(I-R) p53 deletion rescues microcephaly and apoptosis in *Kif20b-/-* brains.

I-L. Coronal sections from E14.5 brains of the indicated genotypes show the severely reduced cortical thickness in *Kif20b* single mutants is rescued by heterozygous or homozygous *p53* deletion. Scale bar: 200 µm.

M. The mean cortical thickness in controls, *Kif20b* single mutants, *Kif20b* mutants with heterozygous p53 deletion, and Kif20b;p53 double mutants is shown. N = 6 *Kif20b+/- p53+/-,* 3 *Kif20b-/- p53+/+,* 4 *Kif20b-/- p53+/-* and 4 *Kif20b-/- p53-/-* mice.

N-Q. Staining for CC3 in cortical sections from E14.5 brains of the indicated genotypes shows increased apoptosis in *Kif20b* single mutants is rescued in Kif20b mutants with heterozygous or homozygous p53 deletion. Scale bar: 20 µm.

R. Mean apoptotic cell density in controls, *Kif20b* single mutants, Kif20b mutants with heterozygous p53 deletion, and *Kif20b;p53* double mutants is shown. N = 3 each of *Kif20b+/ p53+/-, Kif20b-/- p53+/+, Kif20b-/- p53+/-* and *Kif20b-/- p53-/-* mice.

* p < or = 0.05, ** p < or = 0.01, *** p < or = 0.001, **** p < or = .0001. p values calculated with one-way ANOVA. Error bars are +/- s.e.m.

Figure 2: *p53* deletion restores normal production of intermediate progenitors and neurons in *Kif20b-/-* cortex

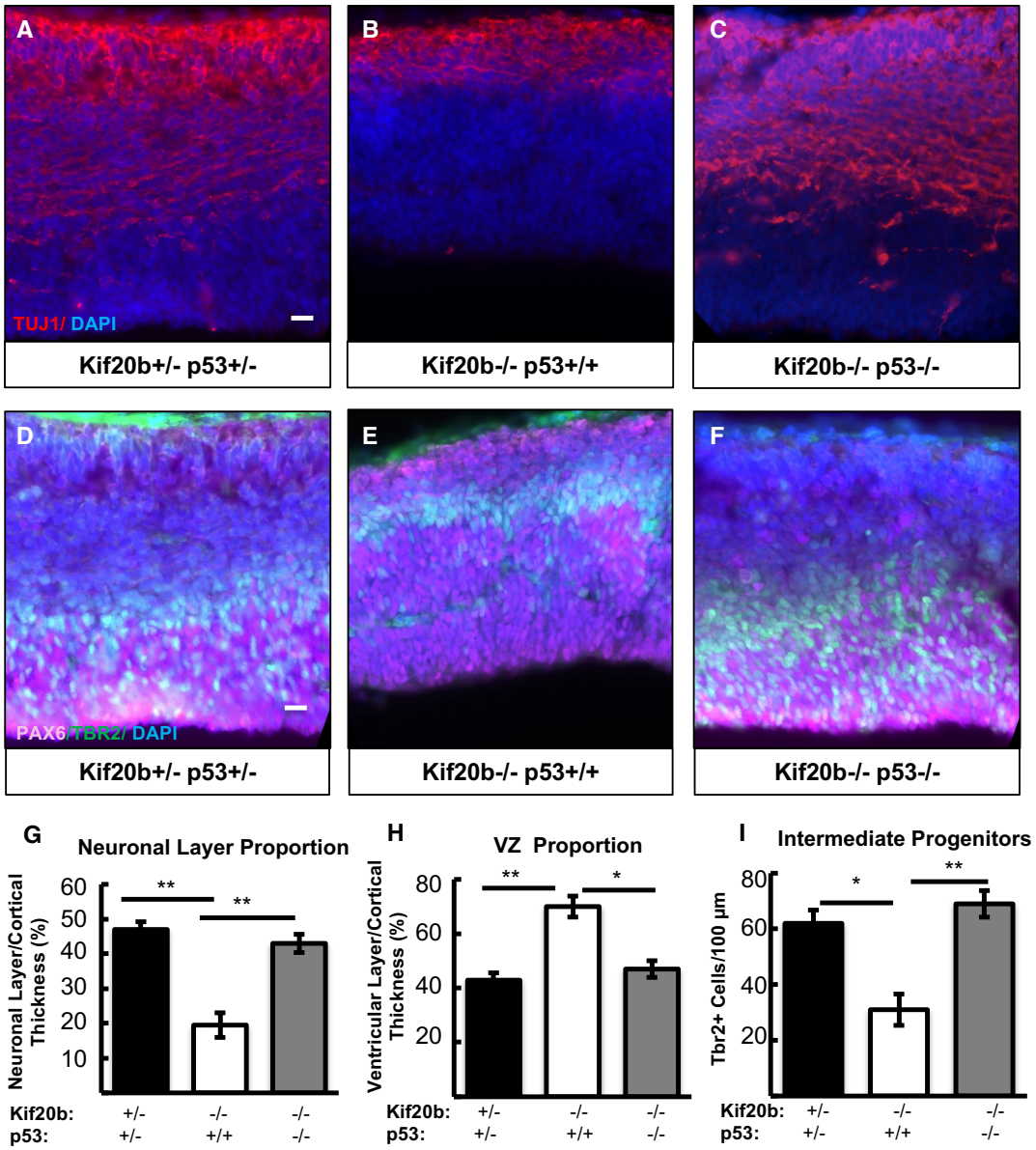

Figure 2: *p53* deletion restores normal production of intermediate progenitors and neurons in *Kif20b-/-* cortex

A-C. Cortical cryosections from E14.5 mice of the indicated genotypes labeled with neuronal-specific tubulin (Tuj1, red) show the decreased thickness of the neuronal layer in *Kif20b* single mutants is rescued in *Kif20b;p53* double mutants. Scale bar: 20 µm.

D-F. Cortical cryosections from E14.5 mice of the indicated genotypes labeled with Pax6 (pink) for NSCs and Tbr2 (green) for intermediate progenitors show the increased thickness of the NSC layer and the decreased number of intermediate progenitors in Kif20b single mutants is rescued in *Kif20b;p53* double mutants. DAPI (blue) stains all nuclei. Scale bar: 20 µm.

G. The mean proportional thickness of the neuronal layer is reduced by approximately half in *Kif20b* single mutants compared to controls but is rescued by *p53* co-deletion.

H. The proportional thickness of the NSC layer, defined by Pax6, is significantly increased in *Kif20b* single mutants, but is rescued by p53 co-deletion.

I. The density of Tbr2+ intermediate progenitors is reduced in *Kif20b* single mutants compared to controls, but is rescued in Kif20b;p53 double mutant mice. N = 3 each *Kif20b+/- p53+/-, Kif20b-/- p53+/+* and *Kif20b-/- p53-/-* mice for neuronal and ventricular layer thickness, and N = 6 *Kif20b+/- p53+/-,* 3 *Kif20b-/- p53+/+* and 4 *Kif20b-/- p53-/-* mice for Tbr2 cell counts. * p < or = 0.05, ** p < or = 0.01. p values calculated with one-way ANOVA. Error bars are +/- s.e.m.

Figure 3: *Kif20b* is required cell-autonomously for cytokinesis of cortical NSCs

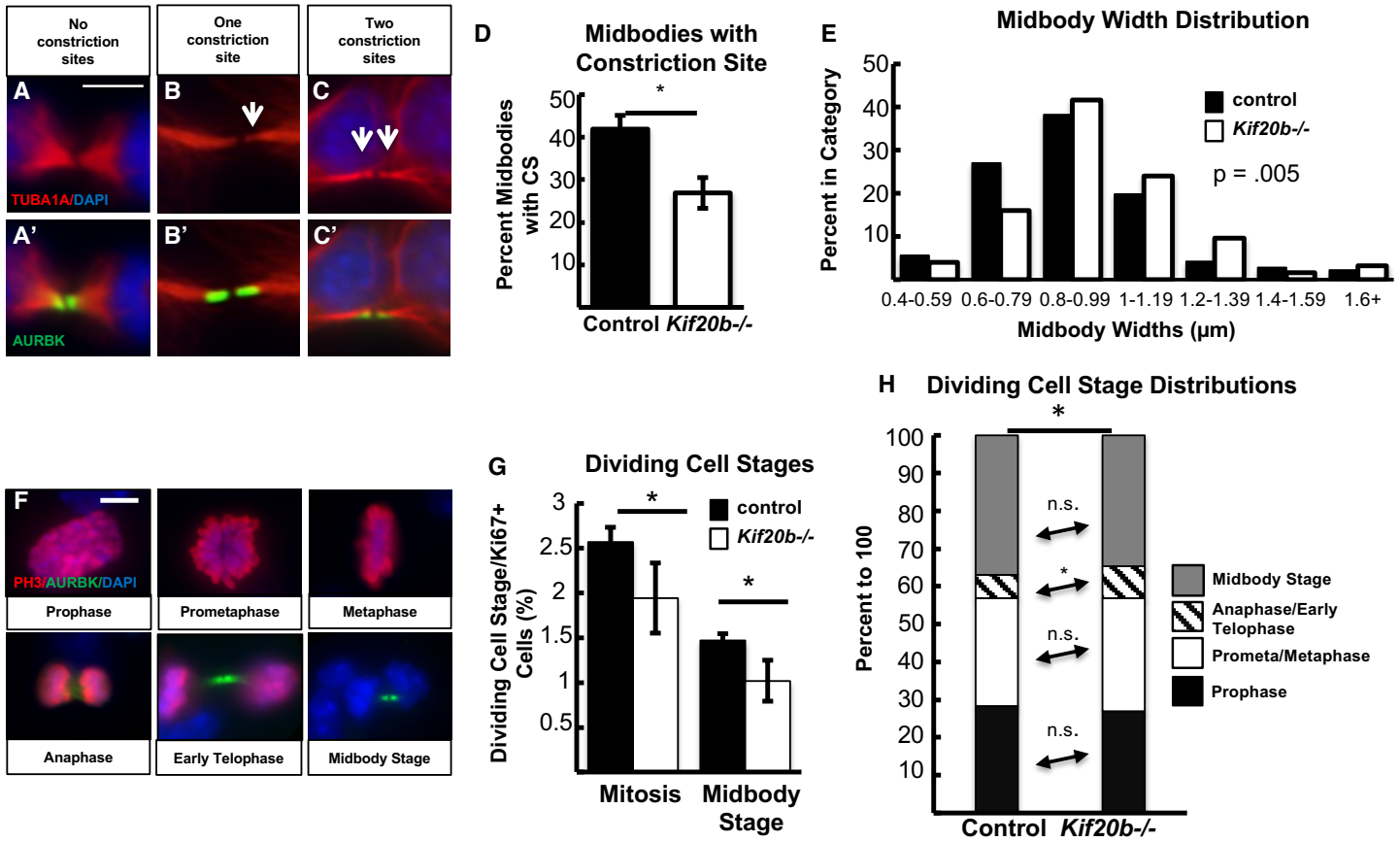

Figure 3: *Kif20b* is required cell-autonomously for cytokinesis of cortical NSCs
A-C. Midbodies of cortical NSCs *in vitro* were labeled with alpha-tubulin, DAPI and Aurora B kinase (red, blue and green, respectively). Early-stage midbodies are wider and have no constriction sites, whereas late-stage midbodies are thinner and have one (B-B') or two (C-C') constriction sites (arrows).
D. The mean percentage of midbodies with at least one constriction site was significantly reduced in *Kif20b-/-* cultures.
E. *Kif20b-/-* midbodies have a shifted width distribution with fewer thin and greater wider midbodies. (Control median = 0.89 µm, mutant median = 0.96 µm). N for graphs (D) and (E): 141 control and 125 midbodies from 6 coverslips and 4 embryos each.
F. Examples of dissociated cultured cortical NSCs in various stages of mitosis and cytokinesis, labeled with PH3 (red, to show mitotic chromatin) and Aurora B kinase (green, to show midbodies).
G. The mean proportions of cycling NSCs (Ki67+ cells) in mitosis or midbody-stage are reduced in *Kif20b-/-* cortical cultures compared to control. N = 3 coverslips from 3 embryos each.
H. Categorizing all dividing NSCs into 4 stages of division, there is a significant shift in the distribution of *Kif20b-/-* NSCs, with increased percentages in anaphase and early telophase. N = 1499 control and 1421 *Kif20b-/-* mitotic and midbody stage NPCs from 3 coverslips and 3 embryos each. * p < or = 0.05. p values were calculated with M.W. test for (E), student's t-test for (D) and (G), and Chi Square and Fisher's exact test for (H). Scale bars: 5 µm. Error bars are +/- s.e.m. All cultures were dissociated from E12.5 cortices and fixed at 24 hours *in vitro*.

Figure 4: *Kif20b* loss activates apoptosis cell-autonomously in proliferating cortical NSCs

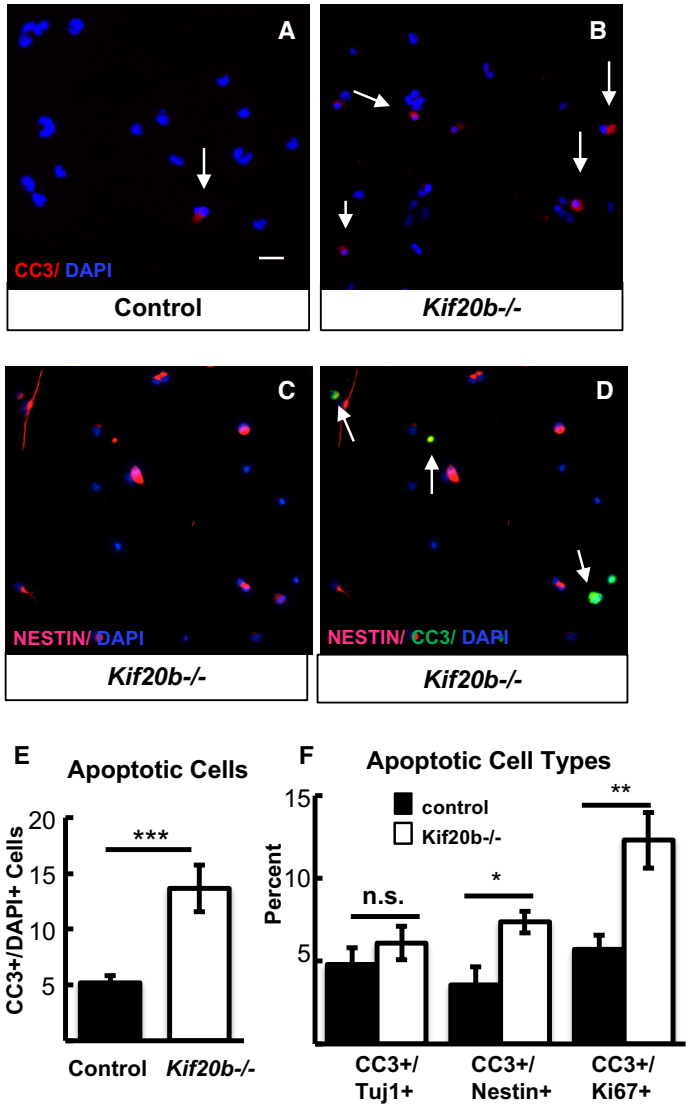

Figure 4: *Kif20b* loss activates apoptosis cell-autonomously in proliferating cortical NSCs
A-B. Representative fields of primary cortical cultures labeled with CC3 (red, arrows) for apoptotic cells and DAPI (blue) for all nuclei.
C-D. Representative fields of primary cortical cultures labeled with Nestin (pink) for NSCs, CC3 (green), and DAPI (blue). Arrows in D indicate cells co-positive for Nestin and CC3 in *Kif20b-/-* cultures.
E. The mean percentage of apoptotic cells in *Kif20b-/-* NPC cultures is more than two-fold increased above controls. N = 13 control and 11 *Kif20b-/-* coverslips from 8 control and 7 mutant embryos.
F. The mean percent of apoptotic neurons (positive for CC3 and Tuj1) in control and *Kif20b-/-* NPC cultures is not significantly different, but the number of apoptotic NSCs (positive for CC3 and Nestin) is significantly increased. Additionally, the number of apoptotic proliferating NSCs (positive for CC3 and Ki67) is increased approximately two-fold. For Tuj1/CC3 analysis: N = 7 control and 6 mutant coverslips from 4 control and 3 mutant embryos. For Nestin/CC3 analysis: N = 7 control and 7 mutant coverslips from 4 embryos each. Ki67/CC3 analysis: N = 6 control and 5 mutant coverslips from 3 embryos each. * $p < 0.05$, ** $p < 0.01$, *** $p < 0.001$. p values were calculated with student's t-tests. Scale bar: 20 µm. Error bars are +/- s.e.m. All cultures were dissociated from E12.5 cortices and fixed at 24 hours *in vitro*.

Supplemental Figure 1: p53 protein level is elevated in *Kif20b-/-* E12.5 brain lysates

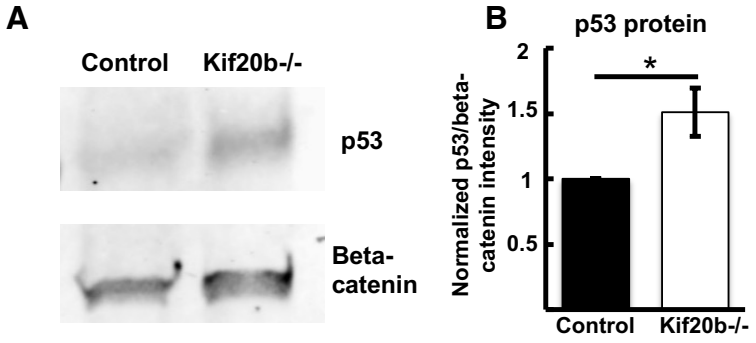

Supplemental Figure 1: p53 protein level is elevated in *Kif20b-/-* E12.5 brain lysates
A. Western blot from E12.5 control and *Kif20b-/-* cortical lysates shows bands for p53 (53 kDa) and beta-catenin (95 kDa) as a loading control.
B. p53 band intensity, normalized to beta-catenin bands, is increased by 50% in *Kif20b-/-* samples. N = 4 western blots from 4 embryos each. * $p <$ or $= 0.05$. p values were calculated by paired ratio t-test.

Supplemental Figure 2: *p53* deletion rescues craniofacial abnormalities in *Kif20b-/-* mice

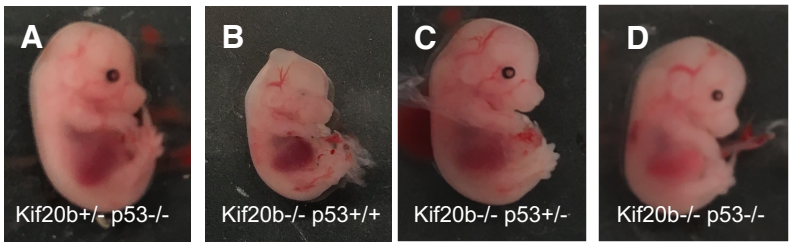

E

Genotype	Percent with craniofacial defects	Percent normal
p53-/- ; Kif20b+/+ or +/-	12% (2/17)	88% (15/17)
p53+/+; Kif20b-/-	100% (3/3)	0% (0/3)
p53+/- ; Kif20b-/-	8% (1/12)	92% (11/12)
p53-/- ; Kif20b-/-	11% (1/9)	89% (8/9)

Supplemental Figure 2: *p53* deletion rescues craniofacial abnormalities in *Kif20b-/-* mice
A-D. E14.5 *Kif20b* single mutant mice have craniofacial defects including underdeveloped eyes, small head, and shortened snout, but heterozygous or homozygous *p53* deletion rescues these defects.
E. Percent of E14.5 mice with each genotype that have craniofacial abnormalities. N = 17 *p53-/- Kif20b+/+* or +/- mice, 3 *Kif20b-/- p53+/+,* 12 *Kif20b-/- p53+/-* and 9 *Kif20b-/- p53-/-* mice.